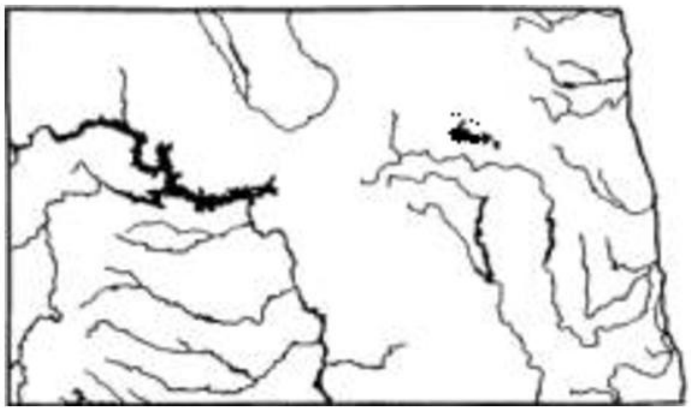

Technical Report No: ND13-01

Toward Understanding the Hydrologic Processes on Topographic Surfaces with Depressions – Modeling and Applications

Jun Yang and Xuefeng Chu
Department of Civil Engineering
North Dakota State University
Fargo, North Dakota

February 2013

North Dakota Water Resources Research Institute
North Dakota State University, Fargo, North Dakota

Technical Report No: **ND13-01**

Toward Understanding the Hydrologic Processes on Topographic Surfaces with Depressions – Modeling and Applications

Jun Yang[1] and Xuefeng Chu[2]
Water Resources Research Institute Fellow[1] and Assistant Professor[2]
Department of Civil Engineering
North Dakota State University
Fargo, North Dakota

February 2013

The work upon which this report is based was supported in part by federal funds provided by the United States of Department of Interior in the form of ND WRRI Graduate Research Fellowship for the graduate student through the North Dakota Water Resources Research Institute.

Project Period: March 1, 2012 – February 28, 2013
Project Number: 2012ND257B
North Dakota Water Resources Research Institute
Director: G. Padmanabhan
Fargo, North Dakota 58108-605

TABLE OF CONTENTS

LIST OF TABLES

LIST OF FIGURES

ABSTRACT

Depressions on topographic surfaces play a significant role in a series of hydrologic processes. However, depressions are rarely simulated in hydrologic models to account for the spatio-temporally varying, discontinuous overland flow due to their complexity. Potholes in the Prairie Pothole Region (PPR) have received increasing attention because of their important roles in water retention, flood control, groundwater recharge and discharge, and water quality management. However, hydrologic functions and behaviors of these potholes are poorly understood due to their spatially and temporally varied hydrologic processes.

In this study, a physically-based distributed puddle-to-puddle (P2P) overland flow model was developed to simulate the dynamic behaviors of depressions and their interactions, and analyze their hydrologic connectivity and the related threshold behaviors. The overland flow model featured with a puddle-based modeling structure and cell-to-cell (C2C) and P2P flow routing procedures. Six simulations were conducted and three experiments were performed in this study to test the P2P overland flow model. Two complex topographic surfaces were selected for hydrologic connectivity analysis by using the P2P model and two modified connectivity indices. In addition, threshold behaviors of potholes were analyzed for a selected watershed in the Red River basin. It is concluded that the P2P overland flow model is capable of (1) quantifying the spatio-temporal distributions and variability of overland flow, (2) characterizing the dynamic depression filling, spilling, and merging processes, (3) simulating infiltration under various topographic surfaces, and (4) revealing the threshold behaviors and hydrologic connectivity under the influence of surface topography.

ACKNOWLEDGMENTS

This research project was primarily supported by the National Science Foundation under Grant No. EAR-0907588. Partial stipend support for the research fellow was provided by the North Dakota Water Resource Research Institute. The authors would like to thank Jianli Zhang, Noah Habtezion, Yingjie Yang, Yaping Chi, Leif Sande, and Daniel Bogart for their contributions to the related modeling and experimental work.

Any opinions, findings, and conclusions or recommendations expressed in this material are those of the authors and do not necessarily reflect the views of the National Science Foundation.

INTRODUCTION

Surface topography influences overland flow generation (Martin et al., 2008), delays the initiation of surface runoff (Darboux and Huang, 2005), and enhances the retention of runoff water (Abedini et al., 2006). In the recent decade, research efforts have been made to quantify the hydrologic role of surface topography, analyze the dynamic behaviors related to surface depressions, and investigate hydrologic connectivity (e.g., Darboux et al., 2001; Darboux et al., 2002; Planchon and Darboux, 2002; Antoine et al., 2009; Thompson et al., 2010). However, more efforts are needed to physically quantify the effects of depressions on surface runoff generation.

Under the influence of surface topography, overland flow can be characterized by a series of hierarchical puddle-to-puddle (P2P) filling, spilling, and merging processes (Chu et al., 2012). Surface depressions play an important role in storing rainwater, controlling overland flow generation and infiltration, modifying runoff patterns, and governing solute transport and soil erosion (Ullah and Dickinson, 1979; Zhang and Cundy, 1989; Huang and Bradford, 1990; Darboux et al., 2002; Darboux and Huang, 2005; Thompson et al., 2010). However, these processes are rarely simulated in overland flow models due to their complexity. Many models rely on removing depressions by smoothing the DEM data (Marks et al., 1984; Jenson and Domingue, 1988) to avoid simulating the complex water movement in depressions and their dynamic interactions. Chu et al. (2012) proposed a new surface delineation approach to characterize surface topography with focus on delineating puddles in a “dynamic” fashion (Chu et al., 2012). The developed puddle delineation (PD) software (Chu et al., 2010) can be used to delineate puddles at different levels, determine their hierarchical relationships, and deal with

special topographic conditions. The puddle delineation results can be further used for the related hydrologic modeling and analysis.

Prairie Pothole Region (PPR) is located in northern United States and southern Canada. It covers the most part of the Red River Basin in North Dakota. The PPR contains roughly 25 million ponds, wetlands and lakes (Gritzner, 2006). The sizes of these depressions or prairie potholes range from an acre to several square miles. Due to their important roles in water retention, flood-peak reduction, groundwater recharge and discharge, and water-quality regulation, these depressions have received increasing attention (Ullah and Dickinson, 1979; Hayashi et al., 2003). Potholes can be characterized by a "fill and spill" process and described as "isolated basins" (Winter and LaBaugh, 2003). In addition, potholes may interact with each other when they are fully filled with water, and they may spill water to their adjacent downstream depressions (Winter and LaBaugh, 2003, Chu et al., 2012). Dynamic storage of potholes showed significant influences on stream runoff response (Spence, 2006). The variability and the dynamic hydrologic processes of depressions have been identified as critical topics to improve the understanding of the hydrology related to prairie potholes (Winter and LaBaugh, 2003). However, hydrologic functions and behaviors of these depressions are poorly understood due to their spatially and temporally varied hydrologic processes (Winter and LaBaugh, 2003), which results in regional hydrologic problems/issues such as water supply, water pollution, and water conflict for agricultural use and natural resources management. Two examples of the regional hydrologic problems in North Dakota are: (1) continuous increase in water level of Devils Lake and (2) frequently occurred floods in the Red River Basin (Gleason et al., 2007).

Hydrologic connectivity has been studied in recent years (e.g., Darboux et al., 2001; Brierley et al., 2006; Bracken and Croke, 2007; Antoine et al., 2009). Hydrologic connectivity has been

used to represent the spatio-temporal conveyance passage to transfer water and the related mass over a land surface (Pringle et al., 2003; Bracken and Croke, 2007). Functional hydrologic connectivity (FHC) characterizes the system responses to dynamic inputs and the complex system structure (Bracken and Croke, 2007). Existing studies on functional hydrologic connectivity focused mainly on analyzing simplified outlet hydrographs (Darboux et al., 2001; Antoine et al., 2009; Appels et al., 2011). However, few efforts have been made to quantitatively reveal the spatio-temporal changes in surface microtopography-influenced hydrologic connectivity.

The study was aimed to: (1) develop a physically-based, distributed P2P overland flow model for simulating the topography-influenced overland flow generation processes and dynamic P2P processes, (2) test the P2P overland flow model by using laboratory experiments, (3) apply the P2P overland flow model to a real site selected in the PPR, (4) analyze the related hydrologic connectivity. The PD software and the P2P overland flow model have been used to: (1) evaluate the DEM resolution effects on surface depression properties (Yang and Chu, 2012a), (2) analyze the spatially and temporally varied hydrologic connectivity (Yang and Chu, 2012b), and (3) quantify the threshold behaviors of potholes in PPR (Chu et al., 2012).

MATERIALS AND METHODS

Development of the P2P Overland Flow Model

Most existing watershed delineation methods rely on filling sinks/depressions so as to define a fully connected drainage network of a watershed. These methods involve detecting the drainage network for a basin by starting from the most upstream cells. It is assumed in the methods that the entire watershed contributes water to the outlet through a well-defined drainage

system and that there is no change in flow directions and accumulations over time (Chu, 2011). Thus, hydrologic modeling based on these delineation methods fails to simulate the dynamic P2P processes and explicitly account for the effects of surface topography on hydrologic processes, such as infiltration and overland flow.

Structure of the P2P Overland Flow Model

Depressions break the continuity and connectivity of topographic surfaces, creating a number of puddle-based units (PBUs). These PBUs often have relatively independent hydrologic characteristics and exhibit strong spatial and temporal variability. Based on the information from the PD program (Chu et al., 2010), the P2P overland model tracks the PBUs for each basin and detects the upstream-downstream contribution relationships of these PBUs to generate a cascaded flow drainage system. PBU is a basic simulation unit in the P2P model, which is characterized with unique threshold behaviors. Each PBU consists of a number of contributing cells and a highest-level puddle that may include a group of lower-level puddles. A PBU connects to its downstream PBU through its overflow threshold. Overland flow is routed for all PBUs by following their sequences in the cascaded flow drainage system.

The cascaded structure of the P2P model facilitates a series of simulations for basins, PBUs within each basin, and puddle-to-puddle and cell-to-cell (C2C) within each PBU (Fig. 1). A DEM-based C2C drainage network is identified for each PBU. In the C2C water routing, water from an upstream area drains to the water-ponded cells in puddles (Fig. 2). The P2P water routing simulates the P2P dynamic processes within a PBU (Fig. 1). If a puddle at the highest level in a PBU reaches its fully-filled condition, the excess water spills to a downstream PBU. The simulation for a basin ends if flow routing is completed for all PBUs in the basin (Fig. 1). The modeling continues for next basin until all basins are simulated. The P2P overland flow

model provides modeling details on the C2C and P2P dynamic processes, puddle filling status, ponded water distributions, discharges at basin outlets, and mass balance for all time steps.

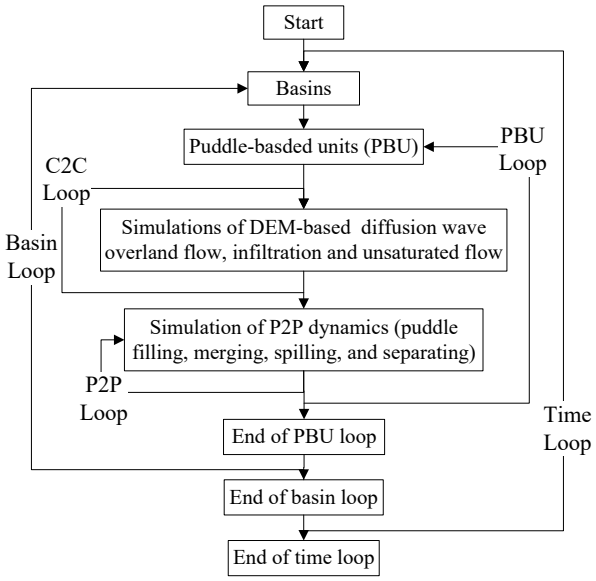

Fig. 1 Simplified flowchart of the P2P overland flow model

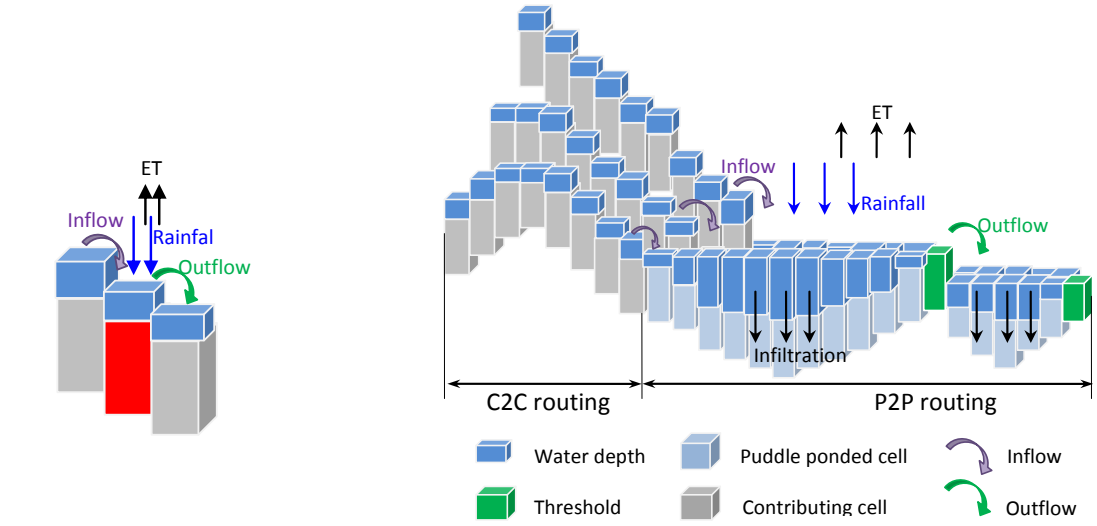

(a) a contributing cell (b) a puddle

Fig. 2 Cell-to-cell (C2C) and Puddle-to-puddle (P2P) flow routing

In the P2P overland flow model, the source terms include lateral inflow and rainfall input while the sink terms consist of lateral outflow, infiltration, and ET losses (Fig. 2). Non-uniform and unsteady rainfall and evapotranspiration can be simulated by specifying a group of rainfall and ET zones. Infiltration is simulated by a modified Green-Ampt model for layered soils under complex rainfall events (Chu and Marino, 2005).

DEM-based Water Routing for Contributing Cells and P2P Dynamic Processes

To physically simulate overland flow on a topographic surface, a C2C drainage network is identified for each PBU. The C2C drainage network of a PBU is a one-dimensional flow system starting from the most upstream cell to downstream cells, and eventually connecting to the puddle(s) corresponding to the PBU. A one-dimensional diffusion wave model (Wang and Hjelmfelt, 1998, and Jain and Singh, 2005) is developed for the C2C flow routing. Research has revealed that diffusion wave equations are sufficiently accurate for modeling overland flow and adequate for a variety of cases of practical interests (Gonwa and Kavvas, 1986; Zhang and Cundy, 1989; Tayfur et al., 1991; Jain and Singh, 2005). The one-dimensional diffusion wave equation can be expressed as:

$$\begin{cases} \dfrac{\partial h}{\partial t} + \dfrac{\partial (uh)}{\partial x} = r - f - e \\ \dfrac{\partial h}{\partial x} = S_0 - S_f \end{cases} \tag{1}$$

where h = water depth; u = depth-averaged flow velocity; x = distance in flow direction; t = time; r = rainfall intensity; f = infiltration rate; e = ET rate; S_0 = surface slope; and S_f = friction slope. The Manning's equation (SI unit system) can be used to calculate flow velocity:

$$u = \frac{1}{n} R^{\frac{2}{3}} \sqrt{S_f} \tag{2}$$

where n = Manning's roughness coefficient; and R = hydraulic radius.

The MacCormack scheme (MacCormack, 1969) is used to solve the diffusion wave equation [Eq. (1)]. The MacCormack scheme has been proven to be one of the most accurate and efficient schemes for overland flow modeling (Kazezyilmaz-Alhan et al., 2004). This solution technique implements a two-step finite difference (FD) scheme (forward FD predictor and backward FD corrector) with second-order accuracy (Wang and Hjelmfelt, 1998). The major advantages of the MacCormack numerical solution method include: (1) it requires fewer parameters; (2) it is feasible, practical, and easily amenable to computer programming; and (3) it provides simulations that have good agreement with those from the full St. Venant equations (Jain and Singh, 2005).

Initial and Boundary Conditions

It is assumed that initially there is no ponded water. Three types of boundary conditions are considered in the P2P overland flow model, including (1) no inflow boundary for the most upstream cells of the delineated overland flow system, (2) constant head boundary for the water ponded cells, and (3) zero-depth gradient boundary for the outlet cells of the surface.

The P2P water routing initiates for a PBU after all water in the C2C drainage network drains to the puddle cells (Fig. 1). The P2P water routing simulates the P2P dynamic processes within a PBU. Two P2P flow routing steps are repeated until all puddles in the puddle routing (PR) list complete their flow routing. If a puddle at the highest level in a PBU reaches the fully-filled condition, the excess water spills to a downstream PBU. After the P2P routing is completed for all puddles in the PR list of the PBU, water routing initiates for next PBU (Fig. 1). Simulation for a basin ends when all of its PBUs complete their flow routing (Fig. 1). The modeling continues for next basin until all basins are routed (Fig. 1). The total discharge from the entire surface is calculated as the sum of discharges from all basins.

The developed P2P overland flow model can be applied to: (1) physically simulate overland flow on rough topographic surfaces, (2) characterize the dynamic P2P filling-merging-spilling-separating processes, and (3) simulate infiltration into soils with various hydrologic/hydraulic properties under complex rainfall events. The model provides modeling details on spatial distribution of overland flow and flow velocity, the P2P dynamic processes, discharges at basin outlets, infiltration and soil moisture conditions, and mass balance summaries for all time steps.

Testing of the P2P Overland Flow Model

Six tests were conducted for the P2P overland flow model. These tests focused on evaluating the P2P model in simulating: (1) the dynamic puddle filling, spilling, merging, and separating processes, (2) infiltration associated with the P2P dynamic processes, and (3) water routing associated with infiltration and the P2P dynamic process. Table 1 shows the details on the parameters used for the six tests, including simulation durations, surfaces, rainfall, soil types, and initial moisture conditions.

Table 1 Parameters of six tests of the P2P overland flow model

Test	Duration (min)	Rainfall intensity (cm/hr)	Surface	Surface size (cm^2)	Experiment	Soil type	Initial soil moisture
1	30.00	1.10	S1	6130.08			
2	80.00	0.10	S2	1211.04			
3	44.00	4.62	S3	6000.00	1	Silty clay	0.165
4	44.00	4.62	S4	6000.00	2	Silty clay	0.165
5	80.00	3.23	S5	36000.00	3	Silty clay loam	0.145
6	19.80	2.0 (15.48 min)	S6	500.00		Silty Clay	0.200

Tests 1 and 2 were conducted for complex topographic surfaces S1 and S2 (Figs. 3a and 3b). The two surfaces were characterized with complex puddle organizations and relationships. They

had 131 and 933 puddles, and 13 and 19 puddle levels, respectively. In the modeling of these two tests, assumptions of instantaneous water transfer and imperviousness were introduced.

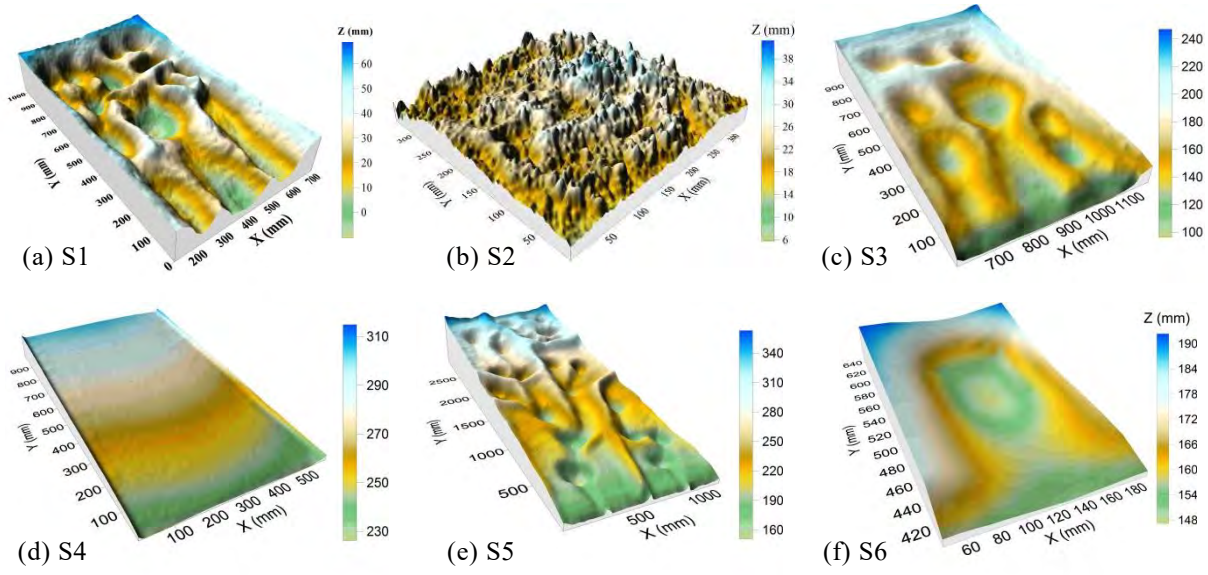

Fig. 3 DEMs of topographic surfaces S1 – S6 for testing the P2P overland flow model

Three laboratory experiments (Experiments 1 - 3) were selected for testing the P2P model. The corresponding tests (Tests 3, 4, and 5) were conducted under the same rainfall and soil conditions (Table 1). Experiments 1 and 2 were conducted for rough and smooth surfaces, respectively (Figs. 3c and 3d), and Experiment 3 was conducted for a larger rough soil surface (1.2×3.0 m^2) (Fig. 3e). These three surfaces (S3 – S5) were scanned by using an instantaneous-profile laser scanner, which created high-resolution DEMs. The rainfall for the three experiments was generated by a four-head Norton-style rainfall simulator. Outlet discharges and the critical times, at which puddles started ponding, merging, and spilling, were recorded during the experiments. Instantaneous water transfer was assumed in the modeling of Tests 3 - 5. The

simulation results were compared with the observed data from the experiments, including outlet discharge, wetting front movement, and occurrence timing of puddle spilling.

Test 6 was conducted for a puddle-dominated surface (S6, Fig. 3f). Surface S6 had an area of 0.05 m^2, featuring a large puddle (Fig. 3f). The simulation period for Test 6 was 19.8 min, and a steady rainfall with an intensity of 2.0 cm/hr and a duration of 15.48 min was applied (Table 1).

Quantification of Topography-controlled Hydrologic Connectivity

Previous studies on functional hydrologic connectivity focused mainly on analyzing simplified outlet hydrographs. New approaches are needed to examine the intrinsic factors that control runoff generation. Hydrographs may not necessarily account for the spatio-temporal variations in the generation and evolution processes of overland flow. Few efforts have been made to reveal the spatio-temporal changes in hydrologic connectivity affected by surface microtopography in an overland flow system. The unique features of the P2P overland flow model allow one to address the issues related to topography-influenced hydrologic connectivity and threshold behaviors. In this study, we also introduced two modified hydrologic connectivity indices to quantitatively describe the spatio-temporal variations in hydrologic connectivity; and evaluate the effects of surface topography on hydrologic connectivity.

P2P Hydrologic Connectivity

Overland flow on a rough surface is characterized by discontinuous P2P filling-merging-spilling-separating dynamics (Chu et al., 2012), which involve a series of hydrologically connected areas (ACs) and individual ponding areas (PAs) under the influence of surface microtopography. Such a hierarchical connecting process is referred to as “P2P hydrologic connectivity” (Chu et al., 2012). Depressions break the connectivity of topographic elements, forming a number of ACs which essentially are the contributing areas for puddles or outlets. An

AC has the potential to expand and connect to its upstream/downstream areas at different stages of overland flow generation. The AC expands when the water level in its puddle reaches the threshold and spills to the downstream area. The outlet hydrograph features a stepwise changing pattern as more areas are connected to the outlet. When all puddles are fully filled, the development of ACs is completed and the entire surface drains runoff water to the outlets. The evolution/formation of ACs leads to dynamic variations in the related hydrologic and geomorphologic processes across the spatial domain. We attempted in this study to quantify the spatio-temporal variability in hydrologic connectivity using the P2P overland flow model by assuming instantaneous water transfer and impervious surface.

Time-varying Hydrologic Connectivity Indices

Based on Western et al. (2001), two modified hydrologic connectivity indices, time-varying connectivity function and connectivity length, were proposed in this study to characterize the statistical properties of ACs and the dynamic changes in ACs across a topographic surface during a rainfall event (Yang and Chu, 2012b). Specifically, a number of ACs with unique ID numbers are identified for each tine step by using the P2P model. Each AC consists of numerous hydrologically connected cells with the same ID. Note that the ID numbers for all cells may change over time due to the P2P dynamics and the evolution of ACs. Based on the ID numbers of cells, the time-varying connectivity function and connectivity length can be respectively computed by:

$$C_{AC}(h,t) = P[i \leftrightarrow i+h \mid ID_{AC}(i,t) = ID_{AC}(i+h,t); i+h \in S; t \in T] \tag{3}$$

$$L_{AC}(t) = \int_0^{\infty} C_{AC}(h,t)\,dh = \sum_{k=1}^{NB} C_{AC}(h_k,t)\cdot \Delta h_k \qquad (t \in T) \tag{4}$$

where $C_{AC}(h, t)$ = connectivity function for separation h at time t; P = probability; $ID_{AC}(i, t)$ = ID number of AC for cell i at time t; h = separation distance; S = space domain that includes all cells; T = time domain ranging from 0 to the end of the time period; $L_{AC}(t)$ = connectivity length at time t; NB = total number of separation bins; h_k = separation distance for separation bin k; and Δh_k = size of separation bin k. The connectivity function index $C_{AC}(h, t)$ represents the lag-dependent and time-varying probability for hydrologic connections between AC-oriented cells across the entire spatial domain. It is expressed as the ratio of the number of pairs of "connected" cells to the total number of pairs for each separation and each time step. The connectivity length index $L_{AC}(t)$ represents the average AC-oriented, time-varying connectivity length for the entire surface.

In addition, ponding connectivity index $C_{PA}(h, t)$ (Chu et al., 2012) was applied to quantify the connections through PAs and characterize the spatial distributions of PAs. The procedures for computing $C_{PA}(h, t)$ were similar to those for $C_{AC}(h, t)$. But it was assumed that the cells within a PA were connected. Similarly, connectivity length of PAs, $L_{PA}(t)$ can be calculated to represent the average connectivity length of PAs.

Combined P2P Experimental and Modeling Study

Experiment 3 (Table 1) and surface S5 (Fig. 3e) were selected for the combined experimental and modeling study on hydrologic connectivity. Discharge was measured at the outlet of the surface. During the experiment, critical times were recorded, at which major puddles started spilling through their thresholds. The experiment was stopped when all puddles were fully filled and the flow system approached to a steady state. Furthermore, the P2P model was applied to simulate the P2P overland flow process under the same conditions (e.g., rainfall, soil, and surface

microtopography). Comparison of the simulation against the experimental data was conducted and in-depth discussions on hydrologic connectivity were performed.

Functional Hydrologic Connectivity Analysis

Two laboratory-scale surfaces (S7 and S8, Fig. 4) were created and used for hydrologic connectivity analysis. Surface S7 (Fig. 4a) was created using a styrofoam board with an area of 0.38 m^2. This surface was characterized with a large number of puddles and complex puddle relationships (e.g., inclusion and upstream-downstream relationships). Surface S8 (Fig. 4b) was generated by randomly distributed soil aggregates across an area of 1.0 m × 0.8 m. High-resolution DEMs of these two surfaces were obtained by using the instantaneous-profile laser scanner. The P2P overland flow model was applied and the proposed connectivity function and connectivity length indices were determined to quantify spatio-temporal variations in hydrologic connectivity of the two surfaces.

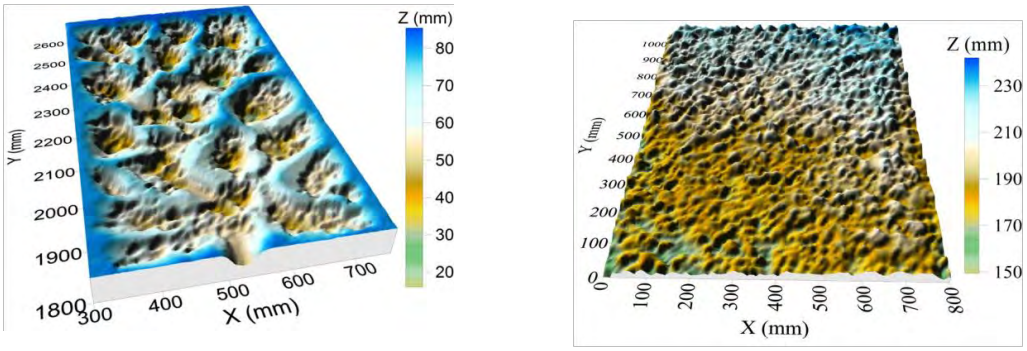

(a) Surface S7 (b) Surface S8

Fig. 4 DEMs of surfaces S7 and S8 for hydrologic connectivity analysis

In this study, functional hydrologic connectivity was analyzed by using three indicators: (1) connectivity function and connectivity length of ACs, (2) connectivity function and connectivity length of PAs, and (3) simplified hydrograph. The first two indicators for FHC characterize the spatio-temporal variations of hydrologic connectivity, while the third indicator provides valuable

information on the overall response of a topographic surface to rainfall inputs at the outlet. Simplified hydrograph denotes the discharge normalized by rainfall input ($r_{Q\text{-}P}$) as a function of cumulative rainfall (CP).

Application of the P2P Overland Flow Model for a Site in the Prairie Pothole Region

To further demonstrate the capability of the P2P overland flow model, a watershed-scale surface (S9, Fig. 5) was selected, which was located in the Red River Basin in North Dakota. The DEM resolution of surface S9 was 10 m. This surface had an area of 8.75×10^6 m^2. The PD program and the P2P overland flow model were utilized for puddle-focused watershed delineation and modeling of the P2P dynamics by assuming instantaneous water transfer and impervious surface. Uniformly-distributed steady rainfall with an intensity of 6.0 cm/hr was applied. The simulation continued until all depressions were fully filled. An initial ponding condition was considered in the modeling for several major wetlands (Fig. 5).

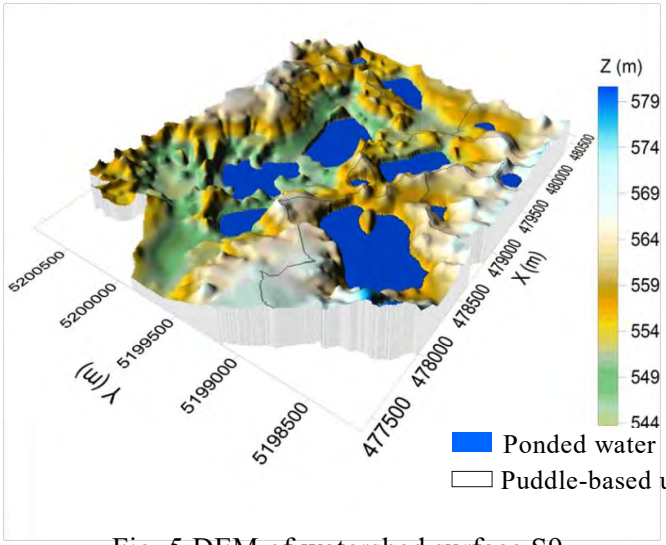

Fig. 5 DEM of watershed surface S9

RESULTS AND DISCUSSION

Tests of the P2P Overland Flow Model

Six tests were conducted for the P2P overland flow model (Table 1). Tests 1 and 2 focused on simulating the dynamic puddle filling, spilling, merging, and separating processes; Tests 3, 4, and 5 were used for testing simulation of infiltration associated with the P2P dynamic processes; and Test 6 demonstrated water routing and modeling of infiltration and the P2P dynamics.

Tests of the P2P Model for Simulating the P2P Dynamics

Fig. 6a shows the simulated water distribution of surface S1 (Fig. 3a) for Test 1 after the entire surface reaches a steady state. Puddle P1 has 39 embedded puddles. Four puddles have an upstream-downstream relationship with P1, as indicated by arrows in Fig. 6a. The contributing area of puddle P1 is 4037.4 cm^2, which accounts 65.86% of the entire surface area. The P2P model simulates the puddle filling, spilling, and merging processes in a dynamic fashion based on the physical relationships and filling conditions of these puddles, as well as rainfall and infiltration characteristics.

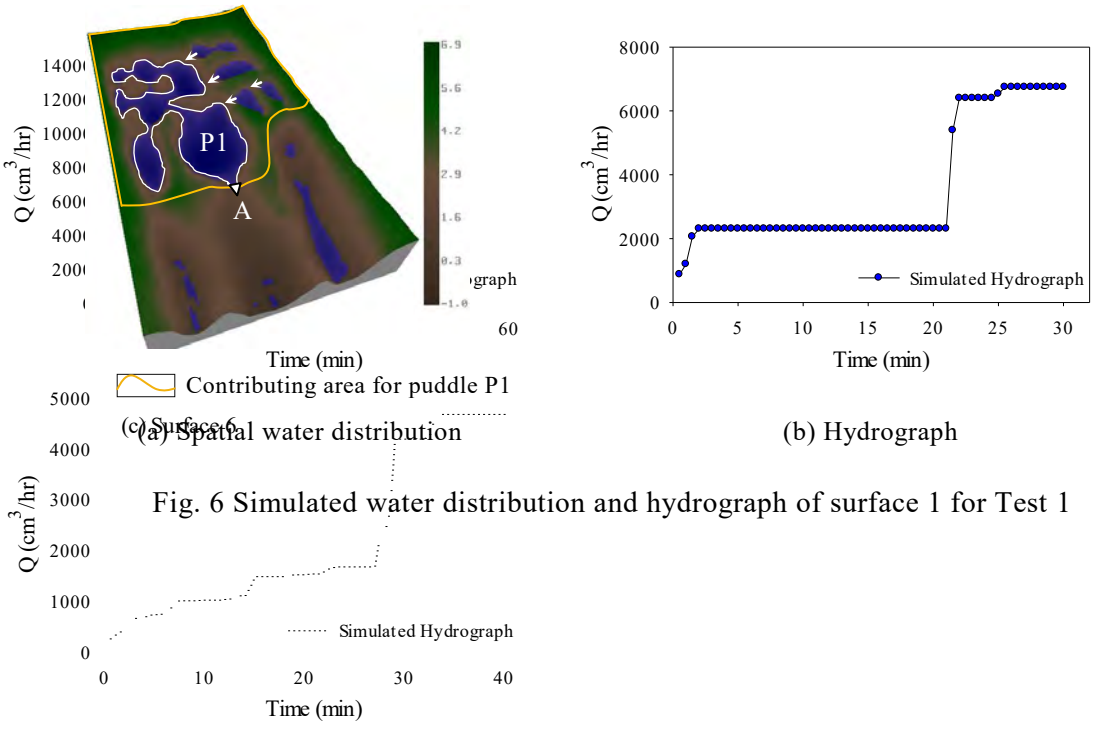

(a) Spatial water distribution (b) Hydrograph

Fig. 6 Simulated water distribution and hydrograph of surface 1 for Test 1

The simulated hydrograph for surface S1 is shown in Fig. 6b. A stepwise changing pattern can be observed. After puddle P1 is fully filled, water spills to the downstream through its overflow threshold (i.e., point A, Fig. 6a), and the drainage system is fully developed, which leads to a significant increase in discharge at t = 22 min (Fig. 6b). Eventually, the hydrograph reaches a constant value.

Fig. 7 shows the spatial distributions of ponded water on surface S2 at four selected times (t = 0, 6, 20, and 110 min). It can be observed that the spatial coverage of ponded water increases and their hydrologic connections are strengthened with an increase in time. Fig. 8 shows the hydrograph of surface S2 from Test 2. A series of stepwise increases can be observed, which can be primarily attributed to the microtopographic features of surface S2. The modeling results demonstrate the capabilities of the P2P overland flow model in simulating the dynamic P2P filling, spilling, and merging processes for complex topographic surfaces.

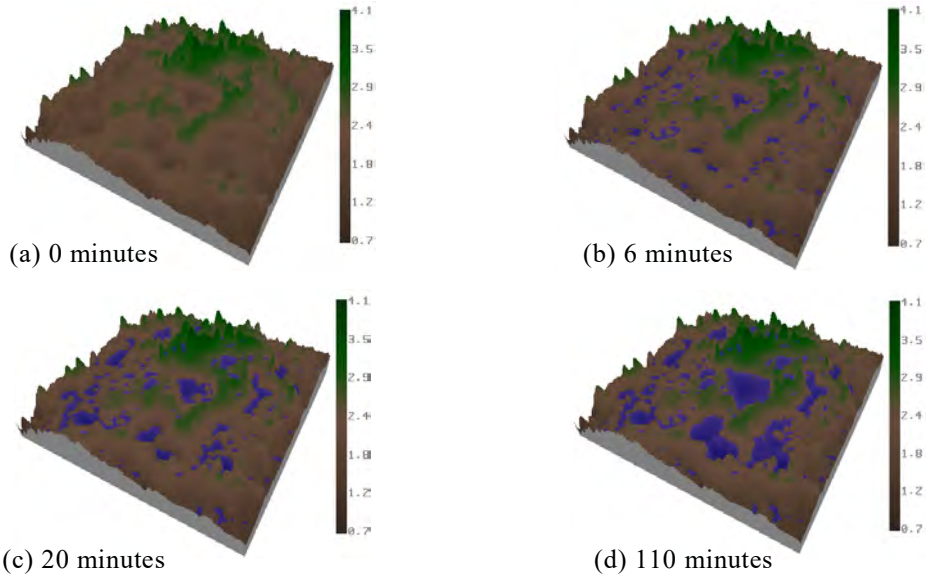

Fig. 7 Simulated water distribution of surface S2 at four different times for Test 2

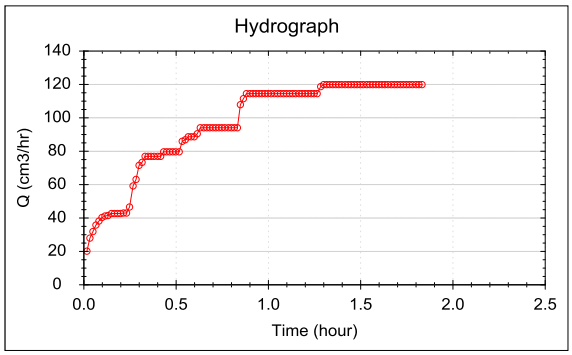

Fig. 8 Simulated hydrograph for Test 2

Tests of the P2P Model in Simulating Infiltration and the P2P Dynamics

Fig. 9 shows the observed and simulated hydrographs for experiments 1 and 2, and the corresponding Tests 3 and 4. These two experiments were conducted for the same soil type (silty clay), rainfall condition (4.62 cm/hr), and initial soil moisture content (0.165) (Table 1). The simulated hydrographs for Tests 3 and 4 match their observed ones from experiments 1 and 2 very well (Fig. 9). The calculated NOF and EF are 0.07 and 0.99 for Test 3 (experiment 1), and 0.08 and 0.98 for Test 4 (experiment 2), respectively.

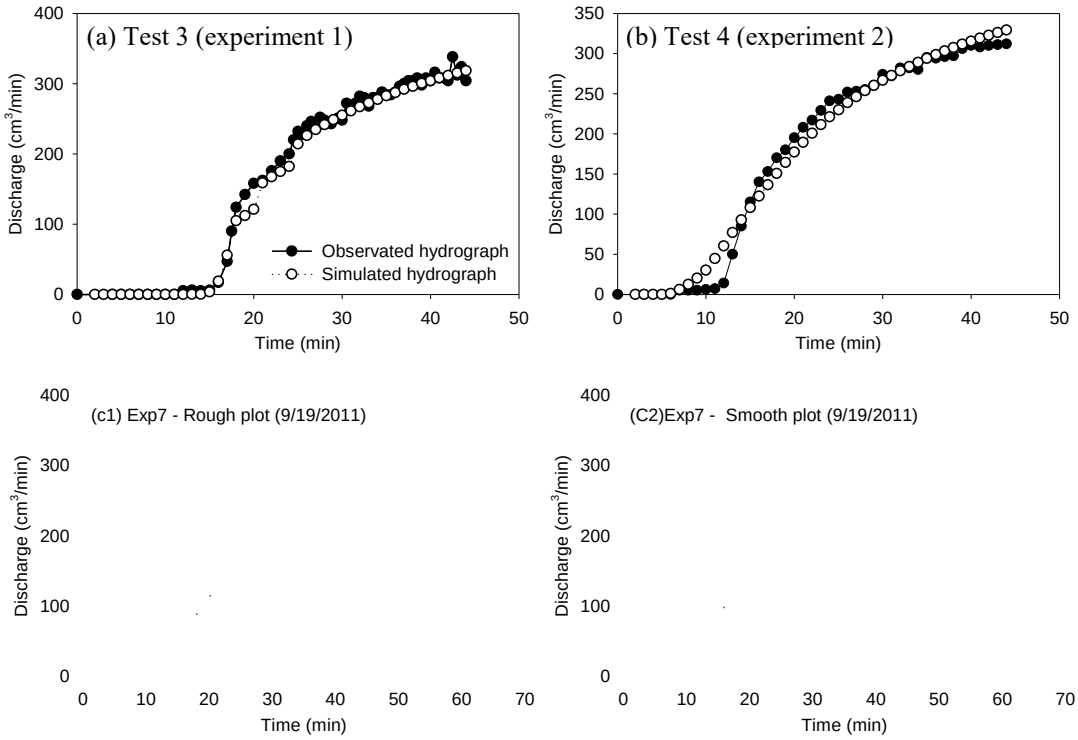

Fig. 10a shows the simulated and observed wetting front curves from experiments 1 and 2, and Tests 3 and 4. Good agreements have been achieved. The calculated NOF and EF are 0.13 and 0.78 for Test 3 (experiment 1), and 0.19 and 0.72 for Test 4 (experiment 2), respectively. The wetting front depths at time 10 and 40 minutes reach 2.05 and 6.85 cm, respectively. The simulated and observed critical times of puddle ponding and spilling for surface S3 are shown in Fig. 10b, from which good agreement also can be observed.

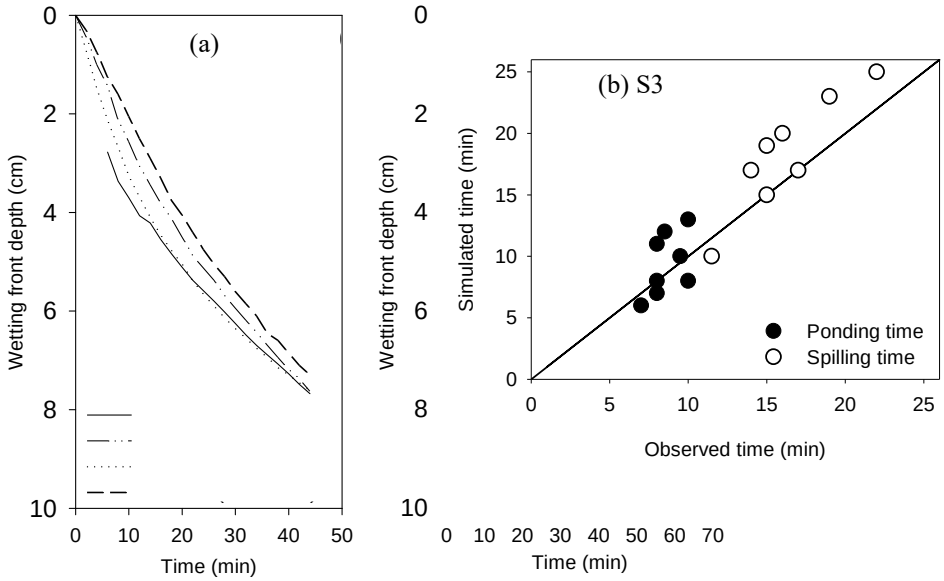

Fig. 10 Comparison of the simulated and observed wetting front depths and critical times for Tests 3 and 4, and experiments 1 and 2

Mass balance analyses for these two experiments and the corresponding modeling tests are summarized in Table 2. Except for the cumulative runoff and infiltration for Test 3, the relative errors for all other mass balance terms are less than 1% (Table 2). It hence can be concluded that good agreements have been achieved for both modeling tests. Infiltration is a dominant process for such a soil system. The observed cumulative infiltration values are 18,403.54 cm^3 (70.89% of rainfall) and 18700.67 cm^3 (70.79% of rainfall) for Experiments 1 and 2, respectively.

Table 2 Mass balance analyses for Tests 3 and 4, and experiments 1 and 2

Mass Balance Terms		Observed	Simulated	Relative Error (%)
Experiment 1 (Test 3)	Cumulative rainfall (cm^3)	25960.32	25960.32	0.00
	Cumulative runoff (cm^3)	6805.00	6612.31	-2.83
	Cumulative infiltration (cm^3)	18403.54	18596.23	1.05
	Depression storage (cm^3)	751.77	751.77	0.00
Experiment 2 (Test 4)	Cumulative rainfall (cm^3)	26417.94	26417.94	0.00
	Cumulative runoff (cm^3)	7717.00	7772.19	0.72
	Cumulative infiltration (cm^3)	18700.67	18645.75	-0.29
	Depression storage (cm^3)	0.28	0.28	0.00

Experiment 3 was used to demonstrate the capability of the P2P model in simulations for a larger and complex soil surface (S5, Fig. 3e). The observed and simulated hydrographs are shown in Fig. 11. The hydrographs again exhibit a stepwise increasing pattern, which can be attributed to the unique threshold flow associated with the puddle filling-merging-spilling dynamics. When all puddles were fully filled, the entire surface contributed runoff water to the outlet through the well-connected drainage system, which led to a significant increase in the hydrographs (Figs. 11).

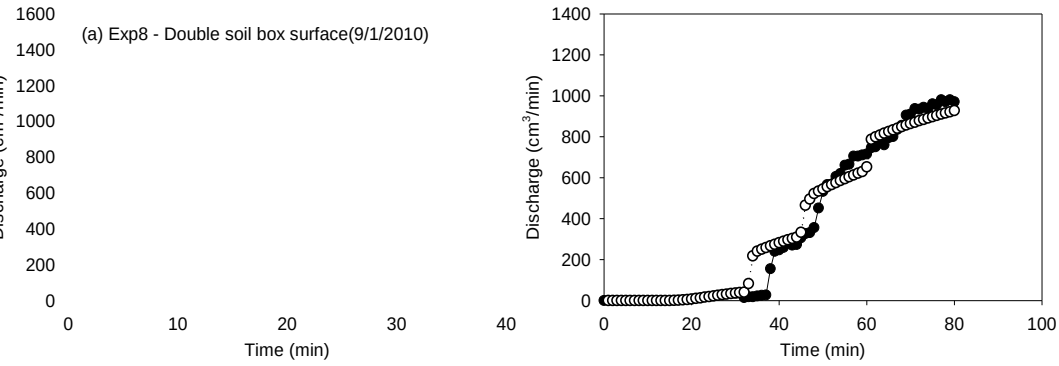

Fig. 11 Comparison of the observed and simulated hydrographs for Test 5 and experiment 3

Comparisons of the simulated and observed wetting front depths and the critical times of puddle ponding and filling processes are shown in Figs. 12a and 12b, respectively. The NOF and

EF for the observed and simulated wetting front depths are 0.15 and 0.97, respectively. Table 3 summarizes the mass balance analysis for Test 5 and experiment 3. The relative error of cumulative infiltration for Test 5 is only 1.01%, which demonstrates the capability of the P2P overland flow model for simulating the topography-influenced infiltration process and the associated P2P dynamics.

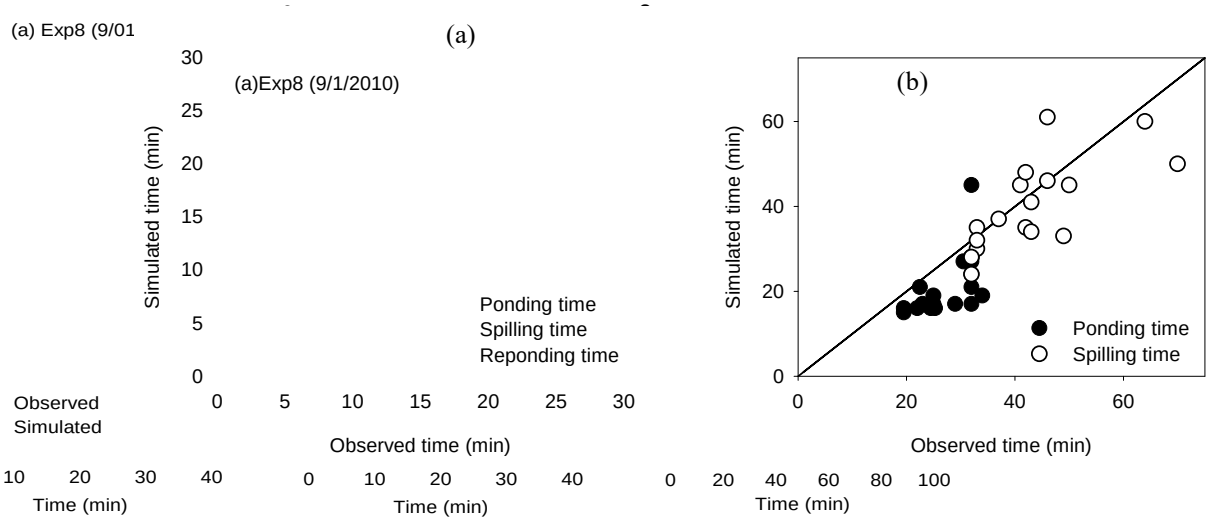

Fig. 12 Comparison of the simulated and observed wetting front depths and critical times for Test 5 and experiment 3

Table 3 Mass balance analyses for Test 5 and experiment 3

Mass Balance Terms	Observed	Simulated	Relative Error (%)
Cumulative rainfall (cm^3)	154896.40	154896.40	0.00%
Cumulative runoff (cm^3)	28361.00	29553.47	-4.20%
Cumulative infiltration (cm^3)	118575.72	117383.25	1.01%
Depression storage (cm^3)	7959.68	7959.68	0.00%

Test of the P2P Model in Simulating Water Routing, Infiltration, and the P2P Dynamics

Test 6 was conducted to demonstrate the capability of the P2P model in simulating overland flow on a puddle-dominated surface (S6, Fig. 3f). Specifically, we tested: (1) the D8 diffusion wave routing approach by using the delineated drainage network for a PBU, (2) the capability of

handling the interactions between diffusion wave routing cells and water-ponded puddle cells, and (3) three types of boundary conditions.

Fig. 13 shows the hydrograph simulated by the P2P model for surface S6 (Fig. 3f). Two stepwise increases can be observed in Fig. 13. The first stepwise increase resulted from the water contribution by the PBU adjacent to the outlet of surface S6. Since there was no puddle in this PBU (Fig. 3f), contributing cells drained water directly to the outlet of the surface. The large puddle on surface S6 underwent a filling process before t = 5.84 min. Overland flow was routed by the diffusion wave model from upstream cells to downstream water-ponded puddle cells in the delineated D8 flow drainage network. The interaction between contributing cells and water-ponded puddle cells was simulated through a constant head boundary condition. The large puddle was full filled at t = 15.88 min, spilling water to its downstream area, which resulted in a significant increase in discharge (Fig. 13). After rainfall stopped, the hydrograph decreased quickly and eventually reached zero. The simulated cumulative infiltration and outlet discharge are 108.06 and 113.10 cm^3, respectively. This test demonstrates the diffusion wave overland flow routing implemented in the P2P model and simulation of the interactions between the contributing cells and the water-ponded puddle cells.

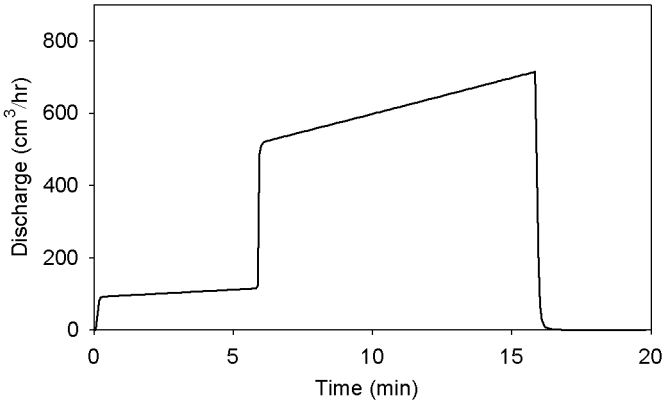

Fig. 13 Simulated hydrograph for Test 6

Topography-controlled Hydrologic Connectivity Analysis

Combined Experimental and Modeling Study for Hydrologic Connectivity Analysis

Fig. 14a shows the observed and simulated hydrographs for surface S5 of experiment 3. Interesting variations in hydrologic connectivity can be observed from the critical times related to initiation of puddle spilling (Fig. 14b) and the calculated connectivity lengths of ACs and PAs (L_{AC} and L_{PA}) (Figs. 14a and 14b). The designed puddle relationships ensured precise measurement of the timing of puddle spilling and observation of the development of ACs and hydrologic connectivity during the experiment. Basically, the puddle ponding and spilling times from the simulation match the observed ones from the experiment (Fig. 14b). The NOF and EF for the simulated and observed times are 0.07 and 0.61, respectively.

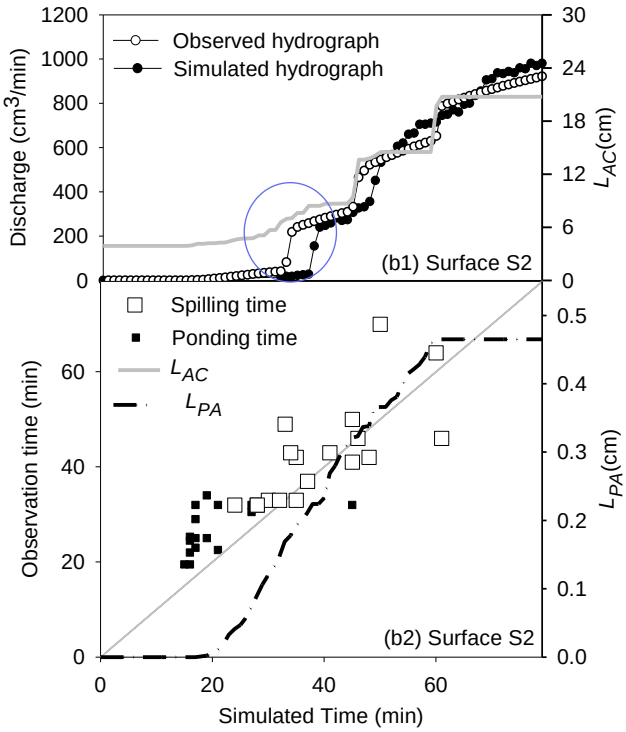

Fig. 14 Observed and simulated hydrographs, critical ponding and spilling times, and connectivity lengths of ACs and PAs (L_{AC} and L_{PA}) for surface S5

The observed and simulated hydrographs start increasing at t = 16.0 min (Fig. 14a). Both hydrographs show a stepwise increasing pattern (Fig. 14a), implying dramatic changes in hydrologic connectivity. A puddle starts spilling once it is fully filled. If its corresponding AC directly connects to the outlet of the surface, a step-wise increase in discharge occurs (Fig. 14a). Each stepwise increase in the hydrograph is associated with a new puddle spilling process and the corresponding evolution of ACs. After all puddles are well connected and the evolution of ACs is completed, the entire surface contributes runoff water to the outlet and the hydrograph reaches a plateau (Fig. 14a).

Simplified hydrograph and connectivity length of ACs (L_{AC}) (Fig. 14a) are two connectivity measurement indicators that have different hydrologic meanings and are calculated by different methods. However, these two indicators show considerable similarity in representing the system response and the behavior of runoff generation. They exhibit a similar stepwise increasing pattern (Fig. 14a). Meanwhile, certain differences can be observed in the shapes of the L_{AC} curve and the simplified hydrograph. L_{AC} is greater than zero at the beginning (i.e., dry surface) (Fig. 14a), which represents the structural hydrologic connectivity property for the surface. Also, L_{AC} shows more detailed stepwise increases or variations, as indicated in the circle in Fig. 14a. This indicates that L_{AC} not only reflects the first type ACs as the simplified hydrograph does, but also is a function of the second type ACs. The difference between the changing patterns of the simplified hydrograph and L_{AC} can be more significant for surfaces with complex topographic characteristics. L_{AC} increases from 3.89 cm (initial stage) to 20.73 cm (final stage) (Fig. 14a). L_{AC} quantifies the properties of both structural hydrologic connectivity (DEM-based hydrologic connectivity of the topographic surface) and functional hydrologic connectivity (P2P hydrologic

connectivity of the dynamic overland flow system). Thus, L_{AC} bridges the gap between SHC and FHC for hydrologic connectivity analysis.

The connectivity length of PAs (L_{PA}) shows a continuous, significant increase before it reaches a plateau (Fig. 14b). Each puddle makes flow contribution to the increase of L_{PA} before it is fully filled. Resultantly, the shape of the L_{PA} curve changes when puddles are fully filled and start spilling in the runoff generation process. The magnitude of L_{PA} at a specific time indicates the average size of the water-ponded areas across the entire surface. The increasing pattern is determined by surface topography and characteristics of the source/sink terms of the drainage system.

In summary, the dynamic P2P processes govern hydrologic connectivity, control surface runoff generation, and alter the flow drainage pattern. Connectivity lengths for ACs and PAs (L_{AC} and L_{PA}) are capable of quantifying the basic topography-associated hydrologic connectivity and the evolution/formation of hydrologic connectivity, and revealing the dynamic threshold behaviors of overland flow generation.

Quantification of the Spatio-temporal Variations in Hydrologic Connectivity for Surfaces with Various Topographic Characteristics

Fig. 15 displays the simulated hydrographs and connectivity lengths of ACs and PAs (L_{AC} and L_{PA}) for surfaces S7 and S8 (Fig. 4). For surface S8, the simplified hydrograph, L_{AC}, and L_{PA} curves have similar changing patterns (Fig. 15b). However, surface S7 has dissimilar changing patterns of these curves (Fig. 15a). This can be attributed to the distinct topographic characteristics and boundary conditions for surfaces S7 and S8. Surface S7 has larger combined puddles and a close boundary, while surface S8 features smaller uniformly-distributed puddles and an open boundary. Thus, surface S7 has a faster development of hydrologic connectivity

within the topography-influenced system comparing with the development of connectivity to its outlets (i.e., simplified hydrograph).

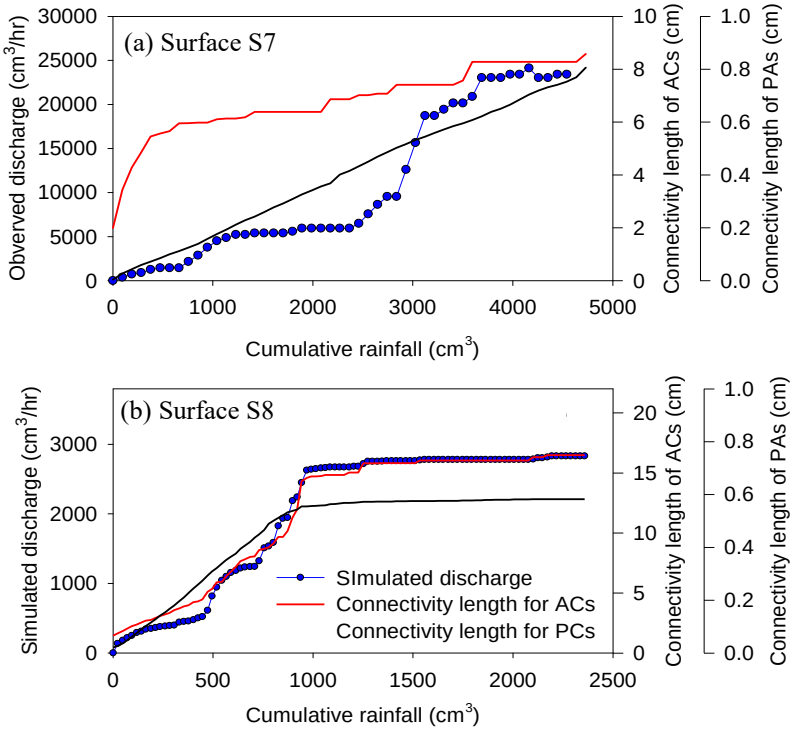

Fig. 15 Simulated hydrographs and connectivity lengths of ACs and PAs (L_{AC} and L_{PA}) for surfaces S7 and S8

The connectivity functions of ACs and PAs of surface S8 for five time points (t = 0.01, 0.08, 0.17, 0.42, and 0.83 hr) are shown in Figs. 16a and 16b, respectively. For any selected time, the C_{AC} curve shows a gradually decreasing trend with separation h (Fig. 16a), which indicates a decreasing pattern of hydrologic connectivity. Hydrologic connectivity is improved with increasing time. Separation h reaches the maximum at t = 0.83 hr (Fig. 16a). Fig. 16b shows the connectivity functions of PAs for the five selected time points. Based on the simulation results, C_{PA} equals 0.0 at t = 0.0 hr because there is no initial ponded water on surface S8. C_{PA} decreases with separation h for other times and ponded water connectivity is improved over time (Fig. 16b).

For any time, the value of C_{PA} for $h = 0$ represents the ratio of ponded area to the total surface area.

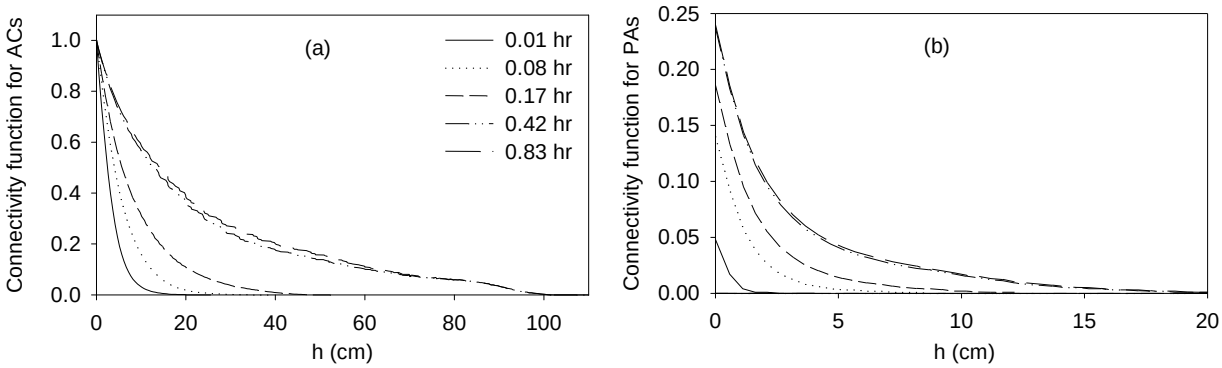

Fig. 16 Connectivity functions of ACs and PAs (C_{AC}, C_{PA}) for surface S8 at different times

It can be concluded from the preceding discussions that the time-varying connectivity functions C_{AC} and C_{PA}, and connectivity lengths L_{AC} and L_{PA} for ACs and PAs effectively reveal the spatio-temporal variations in hydrologic connectivity in the topography-controlled overland flow generation process. Hydrologic connectivity may vary with surface topographic characteristics at different stages of the overland flow generation processes.

Application of the P2P Overland Flow Model in the Prairie Pothole Region

Fig. 17a displays some summarized details on the delineated watershed, including the major highest-level puddles, their thresholds, flow accumulations, and PBUs. Strong non-uniformity can be observed from the shapes and distributions of the delineated puddles. Surface S9 had 204 puddles at 18 different levels. The maximum ponding area and maximum depression storage (MDS) of the entire surface were 2.68 $\times 10^6$ m^2 and 9.95 $\times 10^6$ m^3, respectively. Note that this maximum depression storage did not include the initial ponded water. The main cascaded flow drainage system started from PBU3 and PBU2 to PBU1, and ended at the outlet of the watershed

(point O, Fig. 17a). PBU4 was connected to PBU2, and PBUs 5, 6, and 7 contributed water to PBU3 (Fig. 17a). Note that many small PBUs were combined with larger PBUs in Fig. 17a.

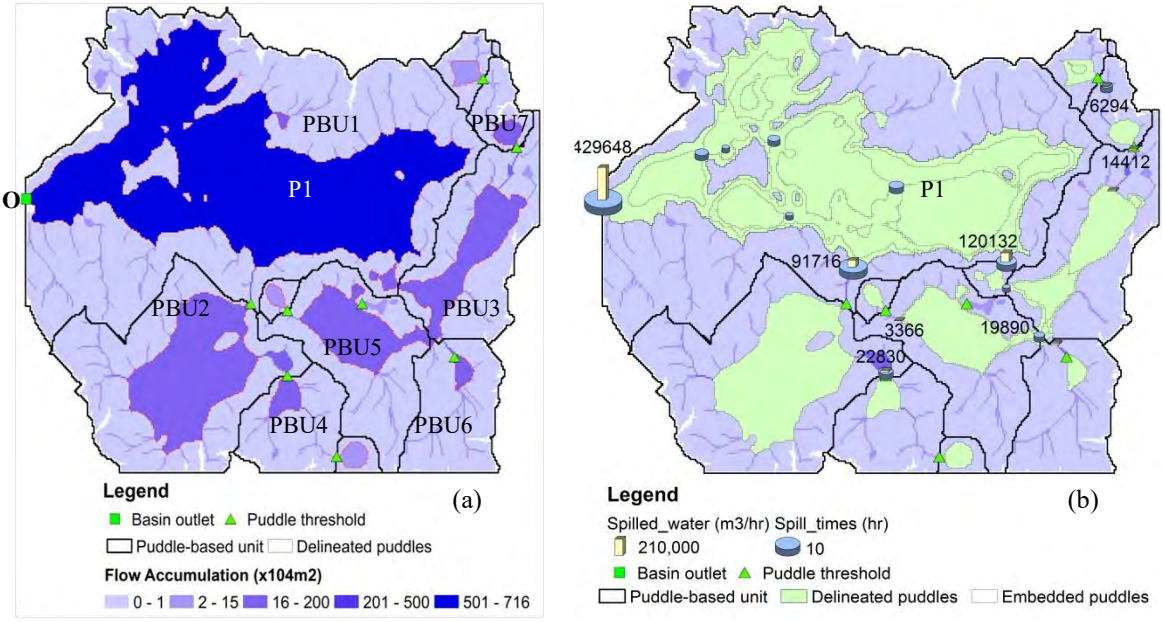

Fig. 17 Delineated puddles and puddle-based units (PBUs), and simulated threshold flow and puddle spilling time for surface S9

A real topography-controlled hydrologic system usually shows complex and dynamic threshold behaviors. The timing of puddle spilling and the amount of spilled water are critical to the related hydrologic analysis. Fig. 17b illustrates the spilling times and the final threshold flow discharges simulated by the P2P overland flow model for all major puddles by assuming instantaneous water transfer. Puddles had dissimilar initial spilling times, depending on their hydrotopographic characteristics (Fig. 17a). Small puddles were fully filled and started spilling at t = 0.33 hr. For large puddles (e.g., P1 in Fig. 17b), however, it took as long as 24.00 hr. The spilling time for a PBU depended not only on its size (area) and the MDS of its puddle(s), but also other topographic features and the lateral inflow from the upstream PBUs.

In addition to puddle filling and spilling, merging also was one of the critical P2P processes within a PBU. PBU1 included 59 puddles at 18 levels, 58 of which were embedded puddles. Following the initial filling and spilling processes, these embedded puddles underwent a series of merging, filling, and spilling processes, which formed a number of higher-level puddles. Such a process repeated until the highest-level puddle was fully filled. Spilling of the embedded puddles in a PBU varied, depending on their filling conditions and their relationships to others. The dynamic P2P processes of the embedded puddles influenced the hydrologic behaviors within a PBU although the embedded puddles made no direct contributions to the overall flow discharge at the outlet of the watershed.

Potholes in the Red River Basin were a series of cascaded, threshold-driven big "puddles" (lakes). Each pothole had its own filling status and interacted with others. Eventually, all PBUs in the P2P drainage system were well connected. As shown in Fig. 17b, the final threshold flow discharges from these PBUs increased along the drainage direction, reaching the highest discharge at the outlet (4.30×10^5 m^3/hr). The P2P overland flow model can be used to simulate the P2P dynamic processes over rough topographic surfaces. The modeling particularly helps understand the detailed P2P filling-merging-spilling overland flow dynamics under the influence of surface microtopography, reveal the actual threshold behaviors, and analyze hydrologic connectivity.

CONCLUSIONS

It has been a challenge to physically simulate the spatially and temporally varying discontinuous overland flow due to their irregularity and complexity. In this study, a physically-based distributed overland flow model was developed to simulate puddle filling, spilling, and merging dynamics, as well as topography-influenced infiltration process. The special features of

this model included a new modeling structure (e.g., puddle-based units) and two water routing procedures (i.e., cell-to-cell and puddle-to-puddle water routing).

Six tests were conducted and three laboratory experiments were used to demonstrate the capabilities of the P2P overland flow model. Based on the testing results, it can be concluded that the P2P overland flow model was capable of: (1) accurately simulating spatio-temporal water distributions and discharge at the outlet(s) of topographic surfaces; (2) modeling the dynamic threshold behaviors of depressions (filling and spilling) and their interactions (merging and spilling); and (3) simulating infiltration under various surface topographic conditions.

In addition, the developed model was further applied to investigate: (1) the topography-controlled hydrologic connectivity and (2) threshold behaviors of potholes in the Prairie Pothole Region. Two modified hydrologic connectivity indices were proposed to quantify scale-dependent and time-varying hydrologic connectivity of connected areas and ponded areas. It was found that connectivity function and connectivity length were capable of quantifying the spatio-temporal variations in hydrologic connectivity. Hydrologic connectivity may vary at different stages of the overland flow generation processes for surfaces with distinct topographic characteristics. Furthermore, the simulation results for a watershed in the Red River Basin demonstrated the capability of the P2P model in simulating the filling, merging, and spilling processes of potholes and revealing their threshold behaviors.

The future study will focus on improving the current P2P overland flow model and applying it to more sites in the Prairie Pothole Region. It is expected to apply the P2P overland flow model to address regional hydrologic issues, such as (1) natural resources management, (2) delineation and modeling of the prairie pothole wetlands, and (3) floods and draughts.

REFERENCES

Abedini, M. J., Dickinson, W.T., and Rudra, R.P., 2006. On depressional storages: The effect of DEM spatial resolution, Journal of Hydrology, 318(1-4), 138–150.

Antoine, M., Javaux, M., and Bielders, C., 2009. What indicators can capture runoff-relevant connectivity properties of the micro-topography at the plot scale? Advances in Water Resources, 32(8), 1297-1310.

Appels, W.M., Bogaart, P.W., and van der Zee, S.E.A.T.M., 2011. Influence of spatial variations of microtopography and infiltration on surface runoff and field scale hydrological connectivity, Advances Water Resource, 34(2), 303-313.

Bracken, L.J., and Croke, J., 2007. The concept of hydrological connectivity and its contribution to understanding runoff-dominated geomorphic systems. Hydrological Processes, 21, 1749-1763.

Brierley, G., Fryirs, K., and Jain, V., 2006. Landscape connectivity: the geographic basis of geomorphic applications. Area, 38(2), 165-174.

Chu, X., 2011. Characterization of Microtopography and its Hydrologic Significance, in Modeling Hydrologic Effects of Microtopographic Features, edited by X. Wang, pp. 1–14, Nova Science Publishers, Inc.

Chu, X., and Marino, M.A., 2005. Determination of ponding condition and infiltration into layered soils under unsteady rainfall. Journal of Hydrology, 313(3-4), 195-207.

Chu, X., Yang, J., Chi, Y., and Zhang, J., 2012. A new method for dynamic puddle delineation and modeling of puddle-to-puddle filling-merging-spilling processes and threshold behavior. Under review.

Chu, X, Zhang, J., Chi, Y., and Yang, J., 2010. An improved method for watershed delineation and computation of surface depression storage. P1113-1122, In: Watershed Management 2010: Innovations in Watershed Management under Land Use and Climate Change, Proceedings of the 2010 Watershed Management Conference, edited by K. W. Potter and D. K. Frevert. American Society of Civil Engineers.

Darboux, F., and Huang, C., 2005. Does soil roughness increase or decrease water and particle transfer? Soil Science Society of America Journal, 69(3), 748–756.

Darboux, F., Davy, P., Gascuel-Odoux, C., and Huang, C., 2001. Evolution of soil surface roughness and flowpath connectivity in overland flow experiments. Catena, 46(2-3), 125-139.

Darboux, F., Gascuel-Odoux, C., and Davy, P., 2002. Effects of surfacewater storage by soil roughness on overland-flow generation, Earth Surface Processes and Landforms, 27, 223–233.

Gleason, R.A., Tangen, B.A., Laubhan, M.K., Kermes, K.E., Euliss, N.H. Jr., 2007. Estimating water storage capacity of existing and potentially restorable wetland depressions in a subbasin of the Red River of the North. U.S. Geological Survey Open File Report 2007-1159. U.S. Geological Survey, Reston, VA.

Gonwa, W.S., and Kavvas, M.L., 1986. A modified diffusion wave equation for flood propagation in trapezoidal channels. Journal of Hydrology, 83, 119-136.

Gritzner, J., 2006. Identifying wetland depressions in bare-ground LiDAR for Hydrologic Modeling, In: 26th Annual ESRI International User Conference Proceedings, San Diego, CA.

Hayashi, M., van der Kamp, G., and Schmidt, R., 2003. Focused infiltration of snowmelt water in partially frozen soil under small depressions. Journal of Hydrology, 270, 214–229

Huang, C., and Bradford, J.M., 1990. Depressional storage for Markov – Gaussian surfaces, Water Resource Research, 26(9), 2235–2242.

Jain, M.K., and Singh, V.P., 2005. DEM-based modeling of surface runoff using diffusion wave equation. Journal of Hydrology, 302(1-4), 107-126.

Jenson, S. K., and Domingue, J.O., 1988. Extracting topographic structure from digital elevation data for geographic information system analysis, Photogrammetric Engineering & Remote Sensing, 54(11), 1593–1600.

Kazezyilmaz-Alhan, C.M., Medina Jr, M.A., and Rao, P., 2004. On numerical modeling of overland flow. Applied Mathematics and Computation, 166, 724-740.

MacCormack, R.W., 1969. The effect of viscosity in hypervelocity impact cratering. American Institute of Aeronautics and Astronautics, N. Y., 69-365.

Marks, D., Dozier, J., and Frew, J., 1984. Automated basin delineation from digital elevation data, Geo-Processing, 2, 299-311.

Martin, Y., Valeo, C., and Tait, M., 2008. Centimetre-scale digital representations of terrain and impacts on depression storage and runoff, Catena, 75(2), 223–233.

Planchon, O., and Darboux, F., 2002. A fast, simple and versatile algorithm to fill the depressions of digital elevation models, Catena, 46, 159–176.

Pringle, C., 2003. What is hydrologic connectivity and why is it ecologically important? Hydrological Processes, 17(13), 2685–2689.

Spence, C., 2006. Hydrological processes and streamflow in a lake dominated water course, Hydrological Processes, 20(17), 3665-3681.

Thompson, S.E., Katul, G.G., and Porporato, A., 2010. Role of microtopography in rainfall-runoff partitioning: An analysis using idealized geometry, Water Resources Research, 46, W07520.

Ullah, W., and Dickinson, W.T. 1979. Quantitative description of depression storage using a digital surface model: II. Characteristics of surface depressions. Journal of Hydrology, 42, 63-75.

Tayfur, G., Kavvas, M.L., Govindaraju, R.S., and Storm D.E., 1991. Application of St. Venant equations for two-dimensional overland flows over rough infiltrating surfaces. Journal of Hydraulic Engineering, 119, 51-63.

Wang, M., and Hjelmfelt, A.T., 1998. DEM based overland flow routing Model. Journal of Hydrologic Engineering, 3(1), 1-8.

Western, A.W., Blöschl, G., Grayson, R.B., 2001. Toward capturing hydrologically significant connectivity in spatial patterns. Water Resources Research, 37 (1), 83-97.

Winter, T.C., and LaBaugh, J.W., 2003. Hydrologic considerations in defining isolated wetlands, Wetlands, 23(3), 532-540.

Yang, J. and Chu, X., 2012a. Effects of DEM resolution on surface depression properties and hydrologic connectivity. Journal of Hydrologic Engineering. Accepted.

Yang, J. and Chu, X., 2012b. Quantification of the spatio-temporal variations in hydrologic connectivity of small-scale topographic surfaces under various rainfall conditions. Under review.

Zhang, W., Cundy, T.W., 1989. Modeling of two-dimensional overland flow. Water Resource Research, 25(9), 2019–35.